CHARACTERIZATION AND MODELING OF THERMAL DYNAMIC BEHAVIOR of AlGaAs/GaAs HBTs

Ke Lu and Xiangdong Zhang
Corporate R&D Center, AMP- M/A-COM Inc.
100 Chelmsford St., Lowell, MA 01853-3294, USA

ABSTRACT: *This study presents a systematic investigation at the first time on the dynamic thermal impedance of AlGaAs/GaAs HBTs. A simple small-signal measurement technique is developed to measure the frequency domain relationship between the dissipation power and the HBT junction temperature. The technique provides a unique measurement tool to analyse device thermal structure, such as die attachment and heat-sink. A multi-section RC circuit is proposed in the paper to describe the thermal impedance. The agreements between measurement and simulation results are excellent. This investigation is useful in terms of modeling HBT self-heating effect and its impact on HBT linearity or other temperature-sensitive performance.*

I. INTRODUCTION:

It is well-known that the thermal effect plays an important role on the performance of AlGaAs/GaAs HBTs. The self-heating effect of HBTs under steady-state condition has been investigated in great details in terms of measuring thermal resistance [1], analyzing thermal stability [2,3], and developing different device structures to reduce the thermal resistance[4]. However, very little research has been done on the dynamic performance of the self-heating effect in HBTs. It has been shown that the dynamic thermal impedance can strongly influence the intermodulation performance of AlGaAs/GaAs HBTs [5]. It should also have similar influence on other linearity specifications such as the spectrum re-growth. In a MMIC circuits, the low-frequency interaction introduced by the self-heating can deteriorate the circuit performance. The power amplifier operating at pulsed bias also need a good understanding on the dynamic thermal impedance. The dynamic thermal impedance does not only influence the nonlinear part of the circuit performance, it also influences the small-signal performance of HBTs such as 1/f-noise [6]. In this paper, a detailed analysis on the dynamic self-heating effect is given. Based on the theory, the dynamic thermal impedance of a HBT has been extracted by using a simple measurement technique. The new technique can also be used to estimate the thermal quality of the die attachment. A multi-section RC network is also proposed in this paper to model the dynamic self-heating effect.

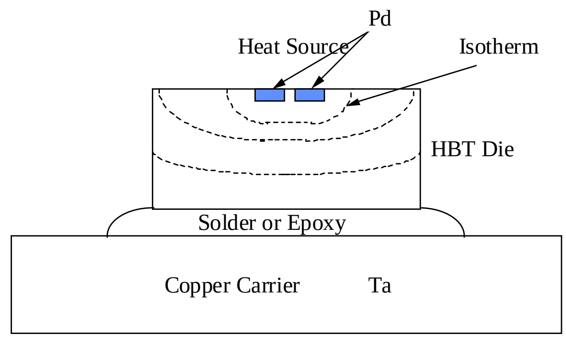

Fig.1 Typical Two-finger HBT mounted on a copper heat sink.

II. BASIC THEORY:

Fig.1 shows a M/A-COM baseline HBT mounted on a copper carrier by using either solder or epoxy attachment. For a HBT under forward operation condition, the power is mainly dissipated inside of the base-collector depletion region. The high-speed carriers give up their energy to the lattice though phonon interactions. This heat generation process is very fast and can be considered as instantaneous. For a HBT with common-emitter configuration (see Fig.2), the terminal current can be described by two nonlinear algebraic equations [7]:

$$I_1(t) = F_1\big(V_1(t), V_2(t), T_J(t)\big) \qquad (1)$$

$$I_2(t) = F_2\big(V_1(t), V_2(t), T_J(t)\big) \qquad (2)$$

for the signal frequency which is low. The junction temperature T_J is determined by the following equations:

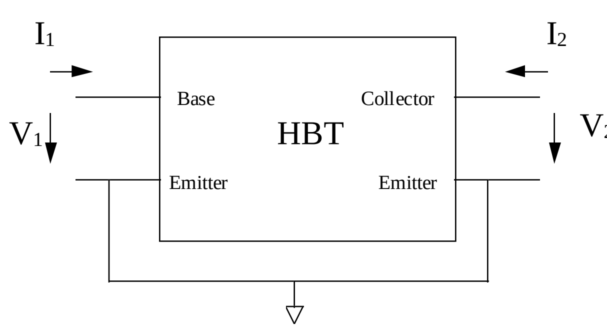

Fig.2 HBT as a two-port network.

0-7803-4471-5/98/$10.00 (c) 1998 IEEE

$$P_D(t)=I_1(t)\cdot V_1(t)+I_2(t)\cdot V_2(t) \tag{3}$$

$$T_J(t)=\int_0^t Z_{TH}(t-t')\cdot P_D(t')\cdot dt'+T_A \tag{4}$$

or $$\Delta T_J(\omega)=Z_{TH}(\omega)\cdot P_D(\omega) \tag{5}$$

where $Z_{TH}(\omega)$ is the Fourier transform of $Z_{TH}(t)$ (we assume a linear thermal impedance for the sake of simplicity and it will not introduce a significant error in most applications).

$$[Y]=\begin{bmatrix} \dfrac{\frac{\partial f_1}{\partial V_1}+\frac{\partial f_1}{\partial T_J}\cdot Z_{TH}(\omega)\cdot I_1}{1-\frac{\partial f_1}{\partial T_J}\cdot Z_{TH}(\omega)\cdot V_1} & \dfrac{\frac{\partial f_1}{\partial V_2}+\frac{\partial f_1}{\partial T_J}\cdot Z_{TH}(\omega)\cdot I_2}{1-\frac{\partial f_1}{\partial T_J}\cdot Z_{TH}(\omega)\cdot V_1} \\ \dfrac{\frac{\partial f_2}{\partial V_1}+\frac{\partial f_2}{\partial T_J}\cdot Z_{TH}(\omega)\cdot I_1}{1-\frac{\partial f_2}{\partial T_J}\cdot Z_{TH}(\omega)\cdot V_2} & \dfrac{\frac{\partial f_2}{\partial V_2}+\frac{\partial f_2}{\partial T_J}\cdot Z_{TH}(\omega)\cdot I_2}{1-\frac{\partial f_2}{\partial T_J}\cdot Z_{TH}(\omega)\cdot V_2} \end{bmatrix}$$

(6)

Based on the equations (1)-(5), the low-frequency small-signal Y parameters of a HBT can be derived (see equation (6)). For a typical microwave HBT with cut-off frequency above 10 GHz, the reactance part of its low-frequency (less than few MHz) Y parameters is purely caused by the thermal impedance. In other word, the Y parameters of a HBT should be nearly resistive for the frequency below few MHz if the measurement can be done at isothermal condition.

III CHARACTERIZATION METHOD AND RESULTS:

An HP 35670A Dynamic Signal Analyzer has been used to measure the Y parameters of HBTs from 1 Hz up to 50 kHz. The setup is carefully designed to ensure the test conditions are fully satisfied. Among four Y parameters, Y22 measurement setup is the easiest one without undue difficulties. For a two-finger HBTs (2x3x10 μm^2), the Y22 values measured at three different current levels are given in Fig.3. In Fig.3, the Y22 traces intercept with the real axis on the right side to form the first intercept points. The first intercept points correspond to the slopes of the output DC IV curves (constant base-emitter voltage bias) for the same HBT at the same current levels measured under non-isothermal condition, (see Fig.4). In Fig.4, the slopes from output IV curves are 0.027, 0.018, 0.0047 (S) at Ic=13, 26, 35 mA, Vc=3 V. In Fig.3, first intercept points for these three conditions are 0.029, 0.017, 0.0053 (S) which agree well with the values from DC measurement. As the frequency increases, these traces rotate clockwise in the complex plane and the Y22's are inductive. These traces should eventually intercept with the real axis again and the second intercept points represent the iso-thermal Y22 values. For a typical AlGaAs/GaAs HBT, the second intercept point should be very close to the original point (0,0) which reflects the fact that the Early voltage is high for AlGaAs/GaAs

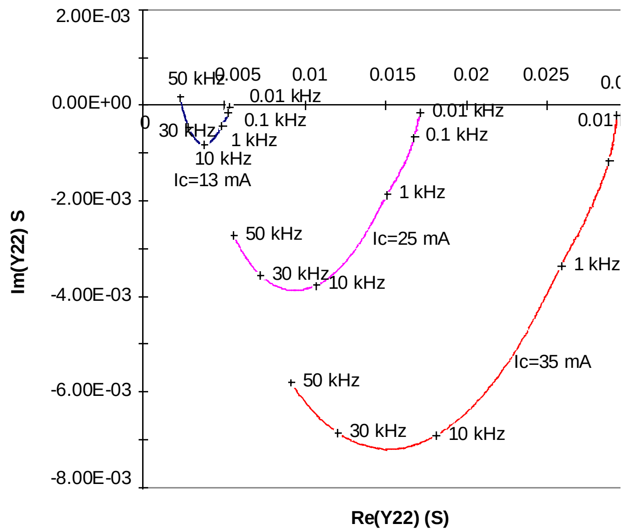

Fig.3 Y22 measurement results at Ic=13, 25, 36 mA, Vc=3 V for a two-finger HBT.

HBTs. Since two coefficients $\partial f_2/\partial T_J$, $\partial f_2/\partial V_2$ can be obtained by the DC test, the thermal impedance can be extracted by using (7).

$$Z_{TH}(\omega)=\frac{Y_{22}(\omega)-\frac{\partial f_2}{\partial V_2}}{I_2+Y_{22}(\omega)\cdot V_2}\cdot\frac{1}{\partial f_2/T_J} \tag{7}$$

In Fig.5, the thermal impedance values extracted from two identical 4-finger HBTs (4x3x20 μm^2) with different die attachments (solder and epoxy) are given as function of frequency. The $Z_{TH}(\omega)$ curve of the HBT with epoxy attachment shows two semi-circles. The first semi-circle intercepts with the second semi-cicle at 100 Hz. The $Z_{TH}(\omega)$ of the HBT with solder attachment only presents one semi-circle. The first semi-circle in epoxy case is caused by the epoxy layer between the die and the copper carrier. Since the epoxy layer has poor thermal conductivity, it simply increases DC thermal resistance by 20% comparing with solder attachment in this case.

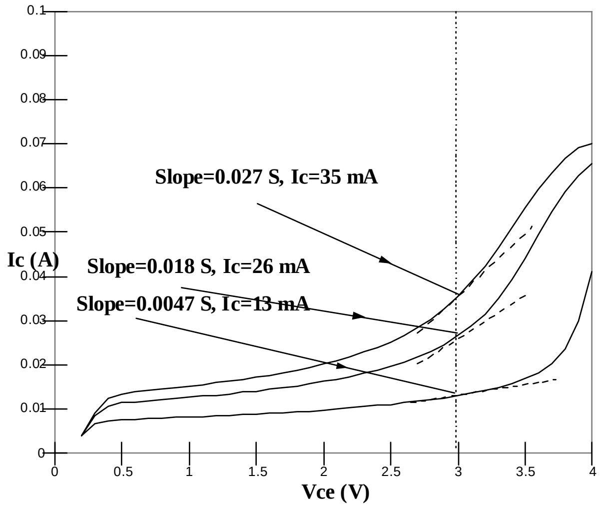

Fig.4, The slopes of three output IV curves corresponding to the same bias conditions in Fig.3 for the same HBT.

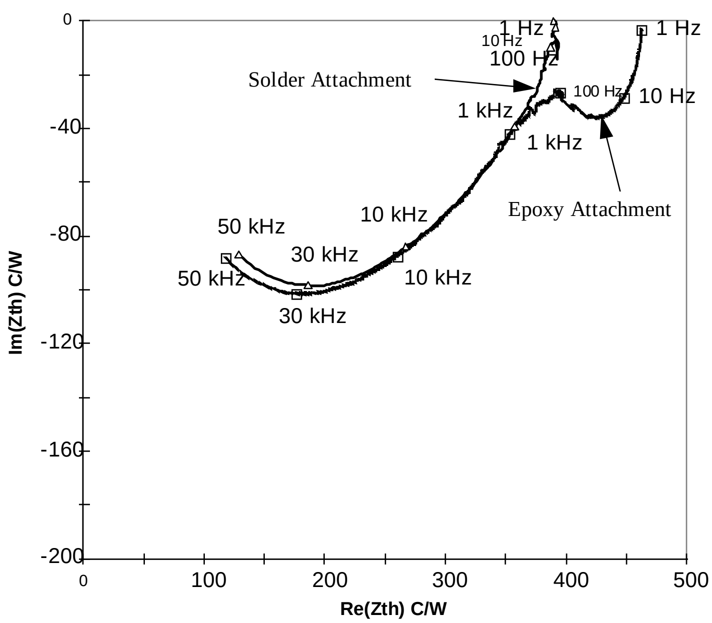

Fig.5 Thermal impedance's extracted from 4-finger HBTs with different die attachments.

When the test signal frequency is higher than 100 Hz, the $Z_{TH}(\omega)$ traces of these two cases are close. This is due to the thermal impedance in high-frequency range

(f>100 Hz) is mainly determined by the size of the die and the thermal properties of GaAs rather than its copper carrier and mounting material. In Fig.5, the difference between two traces can be used to estimate the thermal quality of the die attachment. In the ideal case, the $Z_{TH}(\omega)$ should intercept with the real axis at original point (0,0) when the frequency is high enough (this is the iso-thermal condition where the signal varied so fast and the junction temperature can be considered as a constant and $Z_{TH}(\omega)$ becomes a short circuit). This condition can not be reached easily since the influence of the junction capacitance becomes more significant at higher frequency.

IV. MODELING $Z_{TH}(\omega)$:

The traces of $Z_{TH}(\omega)$ in Fig.5 cannot be approximated by one simple semi-circle since there are multiple thermal time constants in the whole thermal structure, we use a group of simple RC sections in series to approximate the $Z_{TH}(\omega)$, see Fig.6. The node voltage of each RC section represents the temperature on the corresponding iso-therm. The node voltage for the top RC section represents the junction temperature. In general, the top RC section in Fig.6 has the shortest time constant (which means higher R value and lower C value than the section close to the bottom). The more RC sections one uses, the more accurate approximation can be obtained. In many cases, five or six RC sections are enough for most applications. For the 4-finger HBT with epoxy attachment in Fig.5, its $Z_{TH}(\omega)$ can be approximated by 6 RC sections with following values: $R_i = 0.11R_{TH}$, $0.33R_{TH}$, $0.21R_{TH}$, $0.1R_{TH}$, $0.1R_{TH}$, $0.15R_{TH}$; $\tau_i =$ 1E-2, 5E-4, 1E-4, 2.1E-5, 4.2E-6, 1E-7 Sec, where I=1,2,...,6. The slowest time constant is about 1E-2 second which reflects the time constant dominated by the epoxy layer. Fig.7 shows the comparison between measured and modeled $Z_{TH}(\omega)$.

V. CONCLUSIONS:

The dynamic thermal impedance of AlGaAs/GaAs HBTs and its influence on the device performance are investigated in this paper. A simple measurement technique is developed to extract the thermal impedance. The new echnique offers a simple and effective way to analyse the device thermal structure such as die attachment. Multi-section RC network is proposed to model the thermal impedance and the excellent agreement has been obtained between modeled and measurement results.

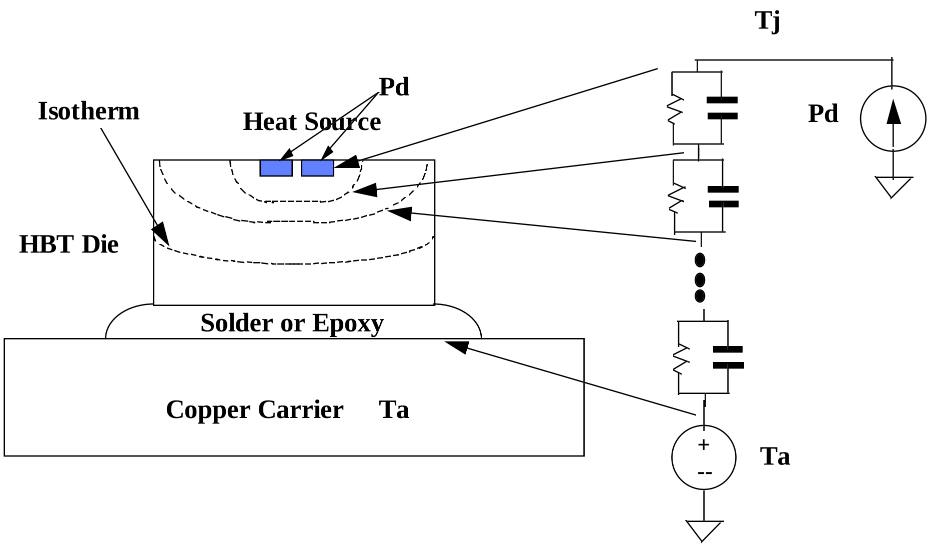

Fig.6 Modeling thermal impedance with multi-RC-sections.

.

ACKNOWLEDGMENTS

The authors would like to thank our HBT teams: A. Hanson, M. Fukuda, C. McLean, Y. Yun, J. Atherton, M. O'Keefe, G. Henderson, P. Ersland, J. Chi for their help. The encouragement and support from Dr. Peter Staecker is greatly appreciated.

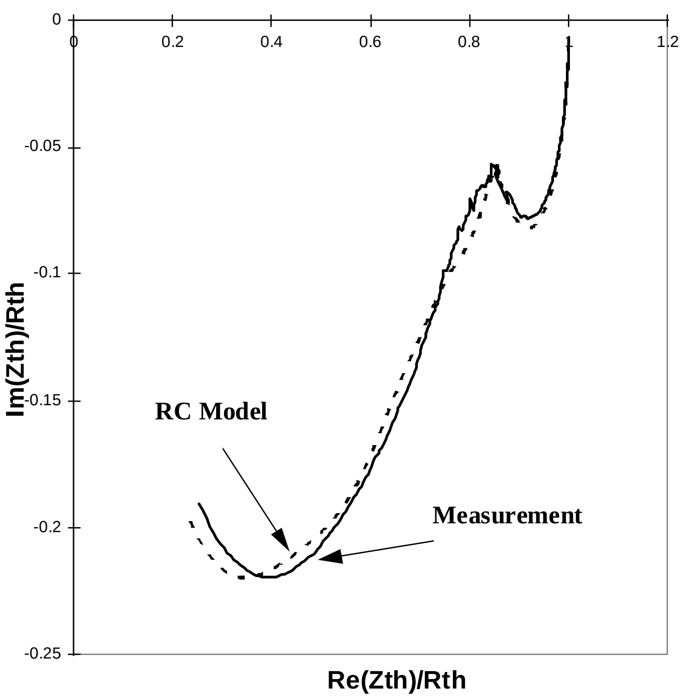

Fig. 7 Comparison between measured and simulated thermal impedance for a 4-finger HBT with epoxy attachment (Note Zth is normalized by Rth).

REFERENCES:

[1] D. E. Dawson, A. K. Gupta, M. L. Salib, "CW measurement of HBT thermal resistance," IEEE Trans Electron Devices, Vol.39, No.10, pp.2235-2239,1992

[2] W. Liu, S. Nelson, D. G. Hill, A. Khatibzadeh, "Current gain collapse in microwave multi-finger heterojunction bipolar transistors operated at very high-power densities," IEEE Trans Electron Devices, vol.40, pp.1917-1926, Nov. 1993

[3] K. Lu, C. M. Snowden, "Analysis of thermal instability in multi-finger power AlGaAs/GaAs HBTs." IEEE Trans on Electron Devices, Vol.43, pp.1799-1805, Nov. 1996

[4] D. Hill, T. Kim, "28 V low thermal impedance HBT with 20W CW output power," 1997 IEEE MTT-S Digest, pp.137-140, 1997

[5] K. Lu, P. M. McIntosh, C. M. Snowden, R. D. Pollard, "Low-frequency disperson and its influence on the intermodulation performance of AlGaAs/GaAs HBTs" 1996 IEEE MTT-S Digest, pp.1373-1376, 1996

[6] O. Muller, J. Pest, "thermal feedback in power semiconductor devices", IEEE Trans on Electron Devices, Vo.17, pp.770-782, Sept. 1970

[7] O. Muller, "Internal thermal feedback in four-poles, especially in transistors", Proc. IEEE, Vol.52, pp.924-930, 1964